Modal analysis and finite element modelling of a grand piano soundboard

Conference Paper · July 2011

CITATIONS
0

READS
143

4 authors, including:

Giacomo Squicciarini
University of Southampton
49 PUBLICATIONS **68** CITATIONS

SEE PROFILE

Proceedings of the 8th International Conference on Structural Dynamics, EURODYN 2011
Leuven, Belgium, 4-6 July 2011
G. De Roeck, G. Degrande, G. Lombaert, G. Müller (eds.)
ISBN 978-90-760-1931-4

Modal analysis and finite element modelling of a grand piano soundboard

R. Corradi[1], P. Fazioli[2], S. Miccoli[1], G. Squicciarini[1]
[1]Politecnico di Milano, Department of Mechanical Engineering, Via La Masa 1, 20133, Milan Italy
e-mail: roberto.corradi@polimi.it, giacomo.squicciarini@mail.polimi.it,
[2] Fazioli Pianoforti, Via Ronche 47, 33077 Sacile, Italy
e-mail: info@fazioli.com

ABSTRACT: The main purpose of this paper is to illustrate the present state of a project aimed at developing and validating a numerical model of a grand piano soundboard. The attention is focused on the comparison between the soundboard vibration modes before and after gluing it to the piano structure. To do so experimental modal analysis campaigns were performed on the soundboard in these two conditions and a finite element model corresponding to the two analyzed construction stages is developed. Peculiarly to the approach adopted, the manufacturing process is reproduced in the model in order to obtain the exact configuration of the soundboard in terms of curvature and internal stresses, since these quantities have an important influence on the vibrational behavior of the soundboard. The final objective will be that of providing support to the entire design process of a new musical instrument.

KEY WORDS: grand piano soundboard, Finite Element, Experimental Modal Analysis.

1 INTRODUCTION

During the last decades the effort of performing experiments in order to validate numerical models capable of reproducing the vibro-acoustic behavior of musical instruments has largely increased and, thanks to the improved calculation power, several interesting results have been obtained. Considering the grand piano soundboard one of the first model presented in the literature is given by Kindel in [1]: by use of a small number of shell and beam Finite Elements, the first few modes of the soundboard were obtained; the piano structure was modeled via beam elements and the results were compared to experiments. Almost ten years later Giordano presented a series of paper (e.g. [2],[3],[4]) about the piano, the results are summarized in [5]; the main idea was to use the Newton's law to create a model of the whole energy flow in the grand piano in the time domain. The soundboard's behavior is modeled solving, via finite difference, the equation of motion of a thin orthotropic plate. More recently Berthaut [6] described the experimental modal analysis campaign performed on a grand piano soundboard in a free boundary condition along with the correspondent Finite Element model. In the paper the numerical results obtained in the modal rage are compared to the experiments and a good correspondence is found up to nearly 250 Hz. Similarly to what presented by Bertahut, the authors of this paper performed an extensive modal analysis campaign; not only the free boundary condition of the soundboard was tested but the modes were identified also when the soundboard is assembled together with the piano case. A Finite Element model of both soundboard configurations was developed.

It is the main purpose of the present paper to present an experimental to numerical comparison for the soundboard having its boundaries both free and clamped. Peculiarly to the approach adopted, the manufacturing process is reproduced in the model in order to obtain the exact configuration of the soundboard in terms of curvature and internal stresses, since these quantities have an important influence on the vibrational behavior of the soundboard. The effort of making an accurate model of the soundboard, considering also its connection to the wood frame of the piano, is of paramount importance if one wants to analyze and model the effects of the manufacturing processes on the tone quality of the instrument.

2 EXPERIMENTAL MODAL ANALYSIS

Experimental modal analysis was performed at different steps during the piano manufacturing process. In this paper attention is focused on the comparison between the soundboard vibration modes before and after gluing it to the piano structure.

In the first case, during the tests the soundboard was suspended with a steel cable (Figure1), so that the soundboard bending vibrations could be considered the same as those of the fully unconstrained structure. The cable length was chosen to set the system first natural frequency below 2 Hz. This choice allowed the sound board rigid motion and its flexible vibration modes to be completely decoupled. In the second case, the test configuration is that reported in Figure 2.

In the case of both Figure 1 and Figure 2, the soundboard was instrumented with 10 piezoelectric accelerometers (sensitivity 100mV/g, measurement range 1000g, bandwidth 10kHz). The excitation was provided by means of two different impact hammers: first a heavy impact hammer with a soft tip allowed an investigation of the low-mid frequency range (0÷1kHz); then the impact tests were repeated using a lighter hammer with an harder tip, to excite the high frequencies, up to about 5kHz. The tests were repeated for two excitation positions and six different accelerometer layouts, corresponding to 60 vibration measurement points in

total, distributed on a square grid with a regular 200x200mm spacing.

Figure 1. Experimental modal analysis: free soundboard.

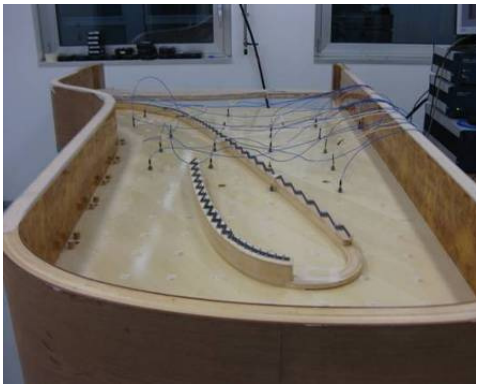

Figure 2. Experimental modal analysis: soundboard assembled on the piano structure.

Only in the case of the soundboard assembled on the piano structure, in addition to the acceleration measurements, an interferometric laser velocimeter was used to scan a 100x100mm grid.

Examples of the measured mobility FRFs are reported in Figure 5 and Figure 6. They respectively refer to the unconstrained soundboard and to the soundboard assembled on the piano structure, for the same combination of excitation position and output vibration measurement point (see Figure 3). Both figures refer to the structure response obtained by exciting the soundboard through the heavier impact hammer and in both cases the measured mobility FRF is plotted in the range 10-1000Hz.

In the low frequency range, were the overlap factor [7] remains below 30%, resonances are clearly spaced and the system shows limited damping. When this condition is satisfied it is possible to efficiently apply standard modal identification procedures. For the tested soundboard, this is the case for the frequency range up to 300-400Hz.

Starting from the measured FRFs, an identification algorithm based on two subsequent steps was applied to identify, for each r^{th} vibration mode, the natural frequency ω_r, the damping factor ξ_r and the mode shape (which is given by the set of modal constants A_{jk}^r corresponding to a fixed excitation point *k* and to variable measurement points *j*).

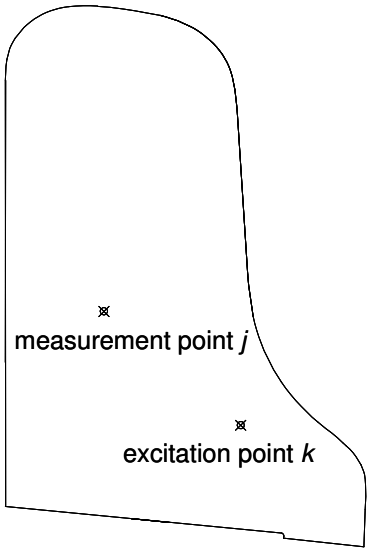

Figure 3. Excitation position and vibration measurement point which led to the FRFs reported in Figures 5 and 6.

In the first step, the time domain LSCE (Least Squares Complex Exponentials) algorithm is applied, to identify initial values of the soundboard natural frequencies and damping factors, in a given frequency range. The system poles are identified considering their stability for increasing model order. An example of stabilization diagram is presented in Figure 4. The poles of the analytical model used to fit the experimental results, are plotted while the order of the model itself is increased. The red circles represent the stable poles, defined as the poles that do not change their frequency and damping factor with respect to the previous iteration, within a certain tolerance. Blue circles are stable only with respect to the frequency, while crosses correspond to non stable poles or noise.

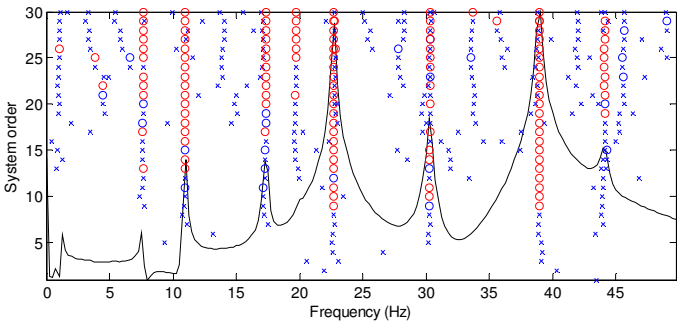

Figure 4. Example of stabilization diagram: the red circles correspond to stable poles.

At the end of the described iterative procedure, the stable values of ω_r and ξ_r are selected and the second step can start, which consists in frequency domain curve fitting. The

system's natural frequencies and damping factors coming from the previous step are considered as initial values and the measured coherence function $\gamma^2(\omega)$ is used as a weighting function in the minimization procedure between experimental and numerical FRFs.

The second step consists in a least squares minimization algorithm, operating in a user-defined frequency band. The adopted FRF analytical model is the following:

$$\alpha_{jk}(\omega) = \frac{1}{\omega^2 M^r_{jk}} + \sum_{r=n1}^{n2} \frac{{}_rA_{jk}}{\omega_r^2 - \omega^2 + 2i\xi\omega\omega_r} + \frac{1}{K^r_{jk}} \qquad (1)$$

To get proper curve-fit, high and low frequency residues (first and third terms in eq. (1), [8]) are added to the contributions of the resonant modes (second term). The residues account for the natural modes out of the identification frequency band.

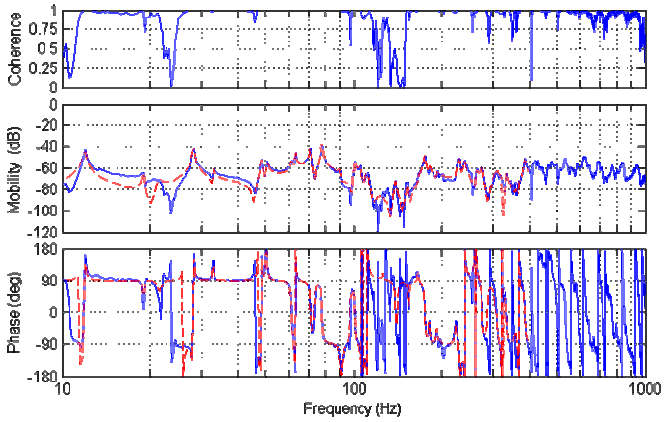

Figure 5. Comparison between experimental (blue) and identified (red) Mobility FRF: free soundboard, excitation and vibration measurement positions as in Figure 3.

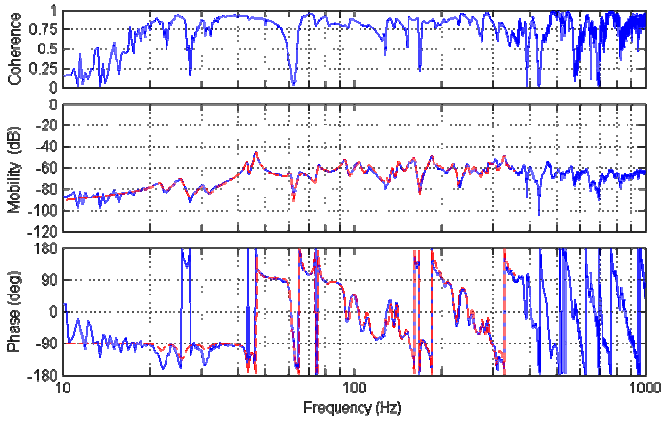

Figure 6. Comparison between experimental (blue) and identified (red) Mobility FRF: soundboard assembled on the piano structure, excitation and vibration measurement positions as in Figure 3.

Figure 5 and Figure 6 show two examples of identified FRFs superimposed to the corresponding experimental ones. The two figures respectively refer to the free soundboard and to the soundboard assembled on the piano structure. By following the described identification procedure, in the first case 39 modes up to 390Hz were identified, while 34 modes up to 350Hz were obtained for the soundboard assembled on the piano structure. In the first case, the identified damping factors vary from 0.4 to 1.0%, in the second case from 0.8 to 3.0%. Examples of identified mode shapes are reported in Figure 10-11-18 and 19

3 FINITE ELEMENT MODEL

Numerical modeling of the soundboard structure was implemented by the Finite Element method using Abaqus/Standard v. 6.9. The present work focuses on the model of the soundboard having free and fully constrained (clamped) boundary conditions along the whole perimeter.

The model is composed of several components: the ribs, the board and the bridges, one for the high tones and one for the low ones (see Figure 7).

The board was modeled using 8 node continuum shell elements (SC8R). This element type was chosen in order to capture exact shell bending behavior with a 3D solid model, and not a 2D mid-surface one. A 3D solid model is very useful for the structure at hand because the board has variable thickness (7 mm at the edges compared to 9 mm at the center) and contact and gluing conditions on both sides, which would be very hard to model accurately by a mid-surface model. Moreover they give better stability in the simulation of the gluing process, in fact they exhibit finite stiffness in the normal direction to the shell surface while classic shell element are perfectly rigid. The board is made up of 6042 elements with an average dimensions equal to 20 mm, this means that the first eigenvalue of each element is approximately equal to 5.1 kHz. In the manufacturing process the board is obtained by edge-gluing several wood strips, in the model this process is neglected and the board is reproduced as an homogeneous plate.

As far as the ribs are concerned, a total number of 20100 solid elements (C3D8R) was adopted, the biggest element having a dimension of approximately 10 mm. The same element type, but with a smaller dimension, is used for the 34500 elements composing the two bridges.

Each component of the structure is made of a different wood. Red spruce is used for the board, Sitka spruce for the ribs and maple for the bridges (a small volume of the bridge is in made of boxwood but to the purpose of a modal analysis of the whole soundboard at low frequencies, the effect of this material can be neglected). The wood is modeled as a homogeneous linear elastic orthotropic material. In order to choose the ten material constants – six elastic moduli, three Poisson's moduli and the density – the authors carried out bending tests measuring the Young moduli E_1 (along the grain direction) and E_2 (in plane direction perpendicular to the grain one) of the Red Spruce and of the Sitka Spruce, the results were then used to tune the data available in the literature (e.g. [9] and [10]). Finally an optimization algorithm is adopted and the wood parameters were refined to increase the experimental to numerical correlation.

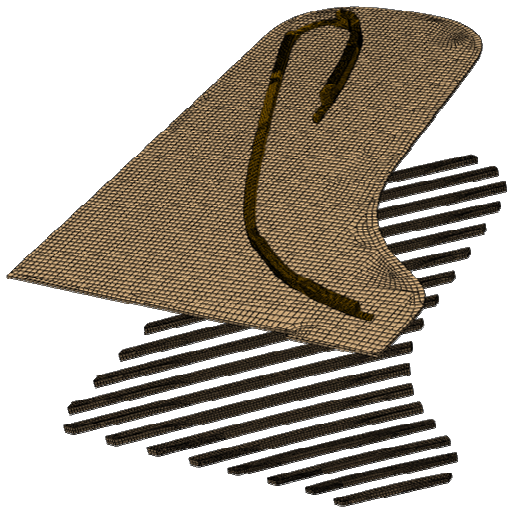

Figure 7. The components of the model: bridges (top), board (mid) and the ribs (bottom).

A grand-piano soundboard is not a flat structure: it exhibits a curvature (called crown in the musical instrument industry) which helps to better withstand the pressure of the strings on the bridges. There are several methods for obtaining the crown, the simplest being gluing a flat board on curved ribs, or, alternatively, exploiting different moisture content between board and ribs at gluing time. For the soundboard under study the so called *compression-crowning* method is adopted: the board and ribs initially are flat and straight, but are glued together under pressure in a curved mold. Pressure is removed after the glue has cured: the board-ribs assembly will not regain its initial shape since no sliding is possible between ribs and board. At the end one has a curved structure with compressive stresses in the board and bending ones in the ribs, hence the name "compression crowning."

Since the actual stress state is hard to guess by other means, in the present study the gluing process was simulated in the FE model by a contact analysis. The ribs are pressed onto the board, which is simply laid down against a curved rigid surface with the mold geometry. The load applied causes the ribs and the board to bend together until the upper surface of the board is completely in contact with the mold. During this phase of the process the surface of the ribs and of the board can mutually slide (unilateral hard contact with no friction on all surfaces). When the applied pressure has reached its final level, the contact interaction between board and ribs is changed to a fully tied one (no separation and no sliding) to simulate the glue bonding. When the applied pressure is set to zero, the soundboard and ribs exhibit an elastic spring-back but the initial planar shape is not regained due to the rib-board mutual constraint. At the end of the simulation the soundboard has a curved shape and the internal stresses (compressive in the board, bending in the ribs) are as expected.

The two bridges are then glued on the upper surface of the board through a similar procedure. The bridges are initially laid down on the upper surface of the soundboard, a distributed pressure is then applied to the top of the bridges and they start to bend until the opening between the bridges lower surface and the board is closed, during this phase sliding between the two contact surfaces occurs. The mold used in the bridges gluing manufacturing process to sustain the soundboard is designed to reproduce the exact soundboard curvature obtained after the ribs gluing. This means that during the loading phase the board is not subjected to any further deformation and the model of the mold is not required. To reproduce this condition several soundboard nodes located nearby the bridges are rigidly constrained to the ground, allowing thus the system to sustain the load. When the loading phase is completed the contact between the bridges and the board is converted to be a perfect tie. Finally the rigid constraints are switched off and, after a slight spring-back, the soundboard gets its equilibrium configuration.

The natural frequencies and mode shapes of the soundboard after bridge gluing are extracted by an eigenvalue analysis taking into account the final geometry and the stress stiffening effects. This results are compared with the experimental results. In order to get more accurate results, the testing conditions were reproduced by modeling the longitudinal stiffness (i.e. ratio between the force and the length) of the suspension steel cable and the mass of the hook. Both elements were simply introduced as a concentrated mass and spring.

The experimental to numerical comparison is represented in term of Modal Assurance Criterion (MAC, eq. (1)) and by comparing the natural frequencies obtained in the two cases.

In equation (1) $\underline{\phi}$ stands for the generic vector of mode shapes, the suffixes *e* and *n* indicate respectively the experimental and the numerical results, while the indexes *i* and *j* vary from one to the number of modes, comparing all the possible combination of numerical and experimental modes.

$$MAC_{ij} = \frac{|\underline{\phi}_{e,i}^T \cdot \underline{\phi}_{n,j}|^2}{(\underline{\phi}_{e,i}^T \cdot \underline{\phi}_{e,j}) \cdot (\underline{\phi}_{n,i}^T \cdot \underline{\phi}_{n,j})} \qquad i,j=1, \ldots, Nmod \qquad (1)$$

The matrix of the MAC is represented in Figure 8, it can be noticed that for 23 modes the index is grater than 0.6 and that the maximum values tend to be on the diagonal of the matrix, indicating that there is an almost one to one correspondence between numerical and experimental modes. Moreover all the experimental modes have an equivalent one in the numerical model and for each one of them the MAC is greater than 0.3.

In Figure 9 the scatter plot of the natural frequencies is showed for the twenty-three modes which have a MAC value greater than 0.6: one can notice that the frequency error is very low and its maximum error is approximately 7%. From this figure the reason for which experimental modes seven and eight are reversed in the numerical model (see Fig. 2) can be inferred. These two modes are in fact very close in frequency and the numerical model, even if it gives the correct mode shape of both, can easily invert the order.

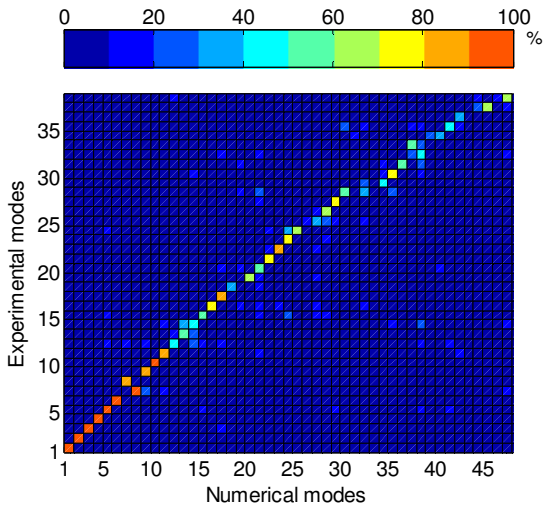

Figure 8. MAC, soundboard in free boundary condition.

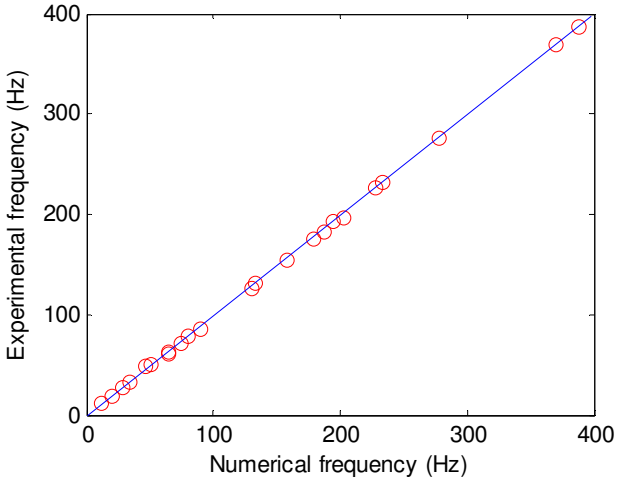

Figure 9. Scatter plot of numerical and experimental natural frequencies of the free soundboard.

Figure 10 and Figure 11 show two examples of identified and numerically computed mode shapes. In Figure 10 on the left side, the experimentally identified mode shape of the third mode is presented. The black small dots in the figure identify the position of the measuring points while the bigger ones mark the positions of the excitation points (the mode shape presented is obtained exciting in the point located towards the treble region). Even though almost 40 modes were experimentally identified without that any spatial-aliasing phenomenon occurred, the measurement grid spacing allows to obtain only a limited number of satisfactory mode shape representations. The matching in the frequency value is, for this mode, really high and the MAC index is greater than 0.9. The twenty-first experimental mode, along with its numerical correspondent one, is presented in Figure 11. The frequency percentage error is equal to 2.2 % and the MAC value is between 0.7 and 0.8.

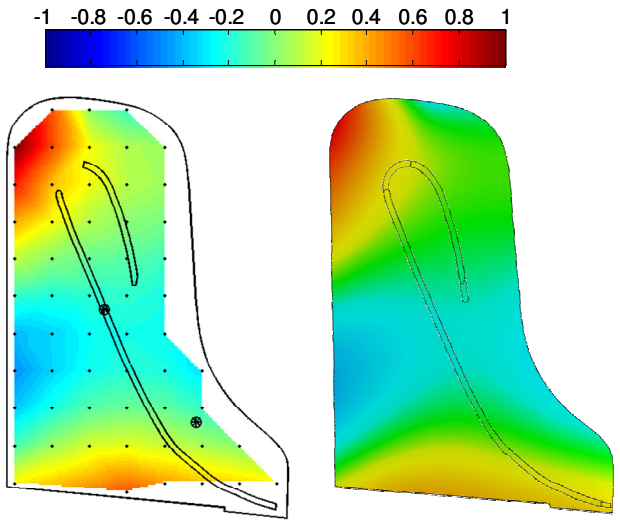

Figure 10. Left: 3rd experimental mode (28.2 Hz). Right: 3rd numerical mode shape: (28.2 Hz).

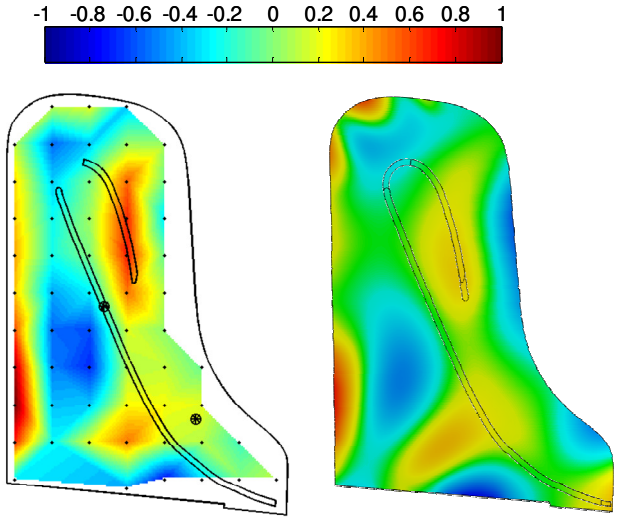

Figure 11. Left: 21st experimental mode (175.4 Hz). Right: 22nd numerical mode shape (179.5 Hz).

After the bridge gluing process the soundboard manufacturing goes on and, before it is glued to the case, the final part of the ribs is planed down to a specific profile. This procedure is done to increase the mobility of the structure and this operation is reproduced in the numerical model too. To do so, the stiffness and the mass of the element modeling the part of the ribs to be removed is set to zero. The internal stresses have to redistribute in the structure and, after a slight deformation, a new equilibrium configuration is attained. In particular, due to the initial stresses configuration (compression for the board) the curvature of the soundboard at the end of the planing down procedure is increased. The portion of the ribs that are removed in the simulation of this process is colored in white in Figure 12. In Figure 13 the color-map shows the relative displacement of the soundboard prior and after the planing.

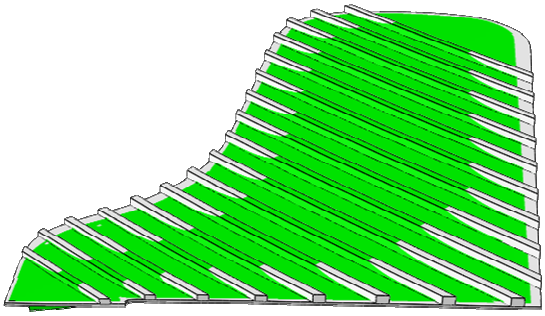

Figure 12. The white part of the model represents the material that is removed during the planing down procedure.

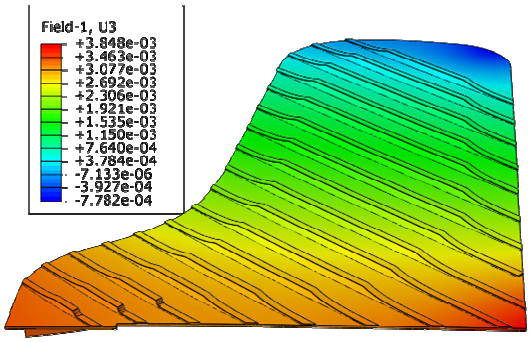

Figure 13. The color-map represents the displacement due to the planing down procedure.

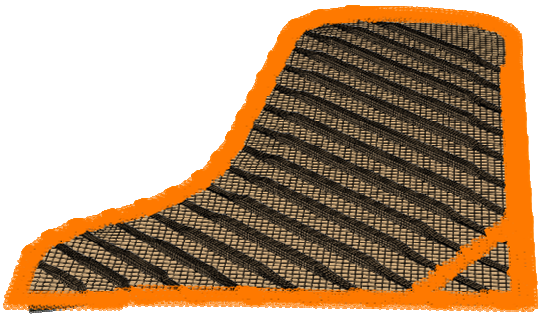

Figure 14. The model is clamped at its boundaries.

The predicted deformed shape of the soundboard was compared to the measured one: the deflection measured at the center of each rib with the same quantity obtained from the numerical model. In Figure 15 this comparison is presented for the seventeen ribs ordered from the treble to the bass region. It is important to point out that the quantities measured on the physical soundboard are affected by a substantial uncertainty due to the flexibility of the soundboard itself: all measurements have to be referred to a reference configuration which is difficult to define and reproduce precisely. Considering this it can be observed that the model is capable, within a reasonable error, of realistically simulating the manufacturing process of the soundboard.

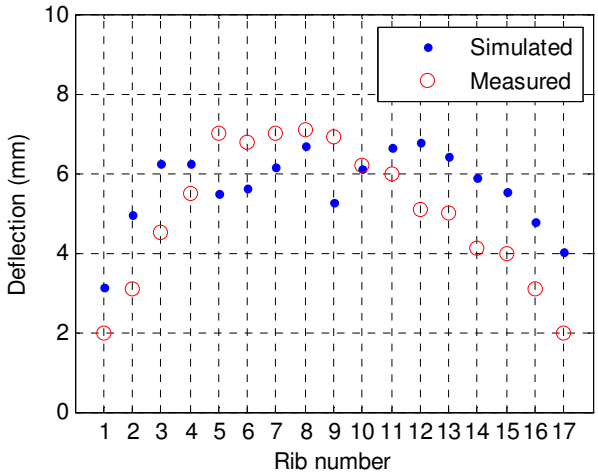

Figure 15. Deflection at the center of the ribs.

In the end if one wants to model the soundboard attached on the piano frame, the simplest methodology is to consider the frame of the piano as a perfect rigid body. Under this assumption it is sufficient to consider fully built-in boundary condition along the whole perimeter. Considering the dimensions and the thicknesses of the frame components with respect to the soundboard, it is not futile to perform a first attempt with this assumption. A set of nodes along the soundboard boundary is therefore rigidly fixed to the ground (see Figure 14) and the eigenmodes are again calculated through a eigenvalue analysis in which curvature and the internal stresses are taken into account. The constrained nodes belong to the surface of the board that is glued to its housing in the case in the real manufacturing process.

In Figure 16 and in Figure 17 the MAC index and the scatter plot of the frequencies are presented for the constrained numerical model and the frequencies and shapes measured on the assembled piano. Observing Figure 16 it is immediately evident that the maxima do not lay on the diagonal of the matrix and, especially for the very first modes, several experimentally identified modes have the same numerical correspondent. It is e.g. the case of the first, of the second and of the third numerical modes, they have clearly at least three experimental correspondents, while the fourth numerical mode has two. At higher frequencies this tendency seems to be less evident but, due to the increased stiffness and damping of the structure, the mid frequency region is reached more rapidly than in the previous case and the experimental modal analysis cannot be successfully performed.

From Figure 17 it emerges an evident inclination for the numerical model to be more rigid than what established in the experiments. Both the results in Figure 16 and in Figure 17 suggest that the choice of a rigid boundary condition for the soundboard is to stiff to obtain good correlations. Modeling the stiffness of the supporting frame is therefore of fundamental importance if one wants to analyze to vibrational behavior of the soundboard. The authors are developing an updated version of the model taking into account also the piano case.

As an example of the results obtained, in Figure 18 and in Figure 19 the mode shapes of the eleventh and of the twenty-sixth experimental modes, along with their numerical

correspondents, are reported. For the first showed mode the MAC index is grater than 0.9, for the latter is between 0.8 and 0.9. In both the cases the numerical frequency is greater than the experimental one.

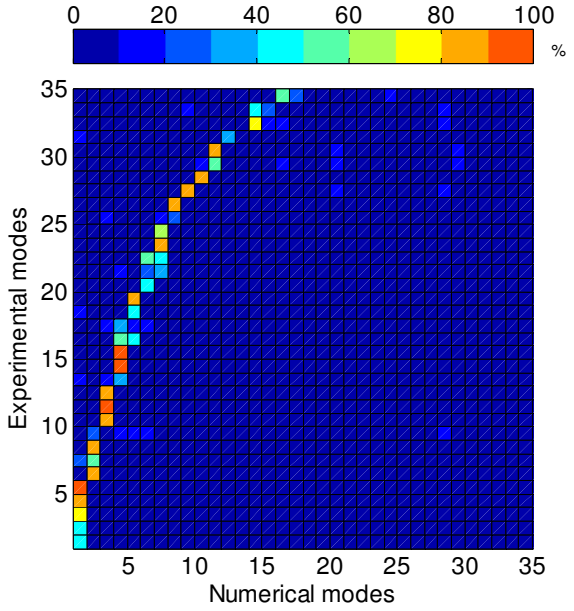

Figure 16. MAC, soundboard in clamped boundary conditions.

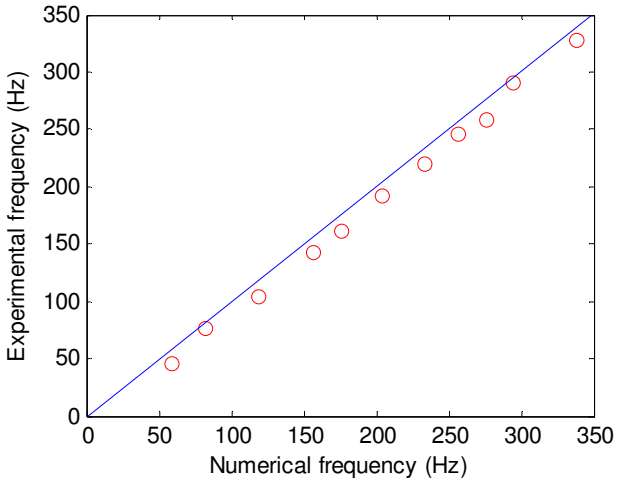

Figure 17. Scatter plot of numerical and experimental natural frequencies of the clamped soundboard.

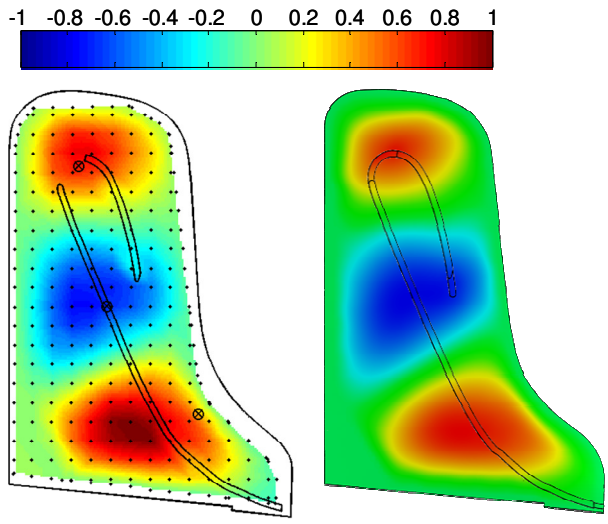

Figure 18. Left: 11th experimental mode shape (103.9 Hz). Right: 3rd numerical mode shape (118.6 Hz).

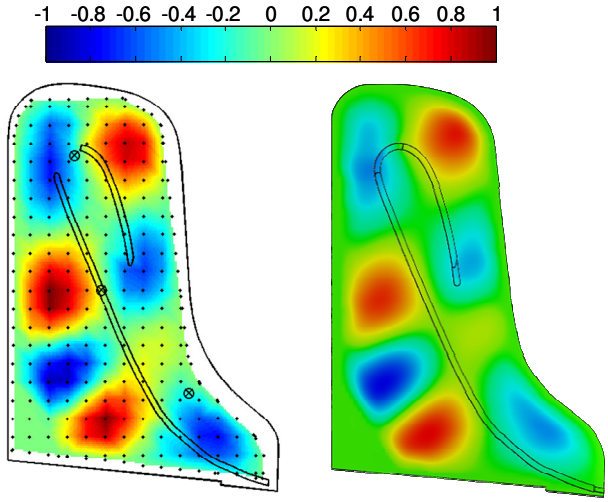

Figure 19. Left: 26th experimental mode shape (219.6 Hz). Right: 8th numerical mode shape (259.9 Hz).

4 CONCLUSIONS

The results obtained from an experimental modal analysis campaign performed on a piano soundboard were used to validate and optimize a finite element model of the structure. Both free and clamped boundary conditions were investigated.

A very good correlation between the experimental and numerical modes has been obtained, for the free boundary condition, up to 400 Hz. On the contrary, in the case of the clamped boundary condition, the finite element model proved to be adequate for reproducing the mode shapes of the soundboard assembled on the piano structure, while the natural frequencies were systematically overestimated. Since this is reasonably due to the piano structure which is not infinitely rigid as assumed in the model, the authors are developing an upgraded version of the finite element model which include the soundboard supporting structure

The research activity is going on and the numerical-experimental comparison will be extended to a higher frequency range. The results obtained will then be used to

develop a model of the sound radiation from the piano soundboard.

The final objective of this vibro-acoustic model will be that of providing support to the entire design process of a new musical instrument.

REFERENCES

[1] Kindel J., Wang I., *Modal Analysis and finite element analysis of a piano soundboard.* In 5th International Modal Analysis Conference (IMAC):1545-1549 1987.

[2] Giordano N., *Mechanical impedance of a piano soundboard.* The Journal of the Acoustical Society of America. 1998;103:2128-2133.

[3] Giordano N., Korty A. J., *Motion of a piano string: Longitudinal vibrations and the role of the bridge.* The Journal of the Acoustical Society of America. 1996;100:3899-3908.

[4] Giordano N., *Simple model of a piano soundboard,* The Journal of the Acoustical Society of America. 1997;102:1159-1168.

[5] Giordano N., Jiang M., *Physical Modeling of the Piano,* EURASIP Journal on Advances in Signal Processing. 2004;2004:926-933.

[6] Berthaut J., *Piano soundboard: structural behavior, numerical and experimental study in the modal range,* Applied Acoustics, 2003;64:1113-1136.

[7] K. Ege, X. Boutillon, B. David, High-resolution modal analysis, *Journal of Sound and Vibration,* 325 (4-5), 852-869, 2009.

[8] D. J. Ewins, Modal Testing: Theory and Practice, Research Studies Press LTD, Great Britain, 1984

[9] Keunecke D., Hering S., Niemz P., *Three-dimensional elastic behaviour of common yew and Norway spruce,* Wood Science and Technolog,. 2008;42:633-647.

[10] Bucur V., *Acoustics of wood*, Springer 2006.